

# Development and application of a diaphragm micro-pump with piezoelectric device

H. K. Ma · B. R. Hou · H. Y. Wu · C. Y. Lin ·  
J. J. Gao · M. C. Kou

Received: 26 June 2007 / Accepted: 29 October 2007 / Published online: 17 November 2007  
© Springer-Verlag 2007

**Abstract** In this study, a new type of thin, compact, and light weighed diaphragm micro-pump has been successfully developed to actuate liquid by the vibration of a diaphragm. The micro-diaphragm pump with two valves is fabricated in an aluminum case by using highly accurate CNC machine, and the cross-section dimension is 28 mm × 5 mm. Both valves and diaphragm are manufactured from PDMS. The amplitude of vibration by a piezoelectric device produces an oscillating flow and alters the chamber volume by the curvature change of a diaphragm. Several experimental set-ups for performance tests in a single micro-diaphragm pump, isothermal flow open system, and a closed liquid cooling system are designed and implemented. The performance of a one-side actuating micro-diaphragm pump is affected by the design of check valves, diaphragm, piezoelectric device, chamber volume, input voltage and frequency. The measured maximum flow rate of present design is 72 ml/min at zero total pump head in the range of operation frequency 70–180 Hz.

## List of symbols

$c$	Damping coefficient
$E$	Module of elasticity
$f$	Frequency
$F$	External force

$g$	Acceleration of gravity
$H_L$	Head loss
$I$	Second moment of area of a rectangular section
$k$	Stiffness constant
$L$	Length of the valve
$M$	Bending moment
$m$	Mass
$P$	Pressure
$t$	Time
$v$	Velocity

## Greek symbols

$\zeta$	Damping factor
$\rho$	Density
$\omega_n$	Natural frequency

## 1 Introduction

Micro-pumps have been developed by using several actuation methods, such as electromagnetic (Böhm et al. 1999), piezoelectric (Stemme and Stemme 1993; Olsson et al. 1996; Koch et al. 1998; Saggere et al. 2000; Suzuki and Yoneyama 2003; Yang et al. 2004; Li et al. 2005), shape memory alloy (Benard et al. 1998), electrostatic (Francais et al. 1997; Teymoori and Abbaspour-Sani 2005), and thermo-pneumatic (Takao et al. 2003) devices. Most of them have complex structures and high power consumption. On the contrary, piezoelectric actuation has advantages of a relatively simple structure and lower power consumption.

Micro-diaphragm pump can be classified as with or without valve. A valve-less pump consists of two fluid flow rectifying diffuser/nozzle elements which are connected to the inlet and outlet of a pump chamber with a flexible

H. K. Ma (✉) · B. R. Hou · H. Y. Wu · C. Y. Lin · J. J. Gao  
Department of Mechanical Engineering,  
National Taiwan University, Taipei, Taiwan  
e-mail: skma@ntu.edu.tw

M. C. Kou  
Cooler Master Co., Taipei, Taiwan  
e-mail: Ken\_Kuo@coolermaster.com.tw

diaphragm. Stemme and Stemme (1993) proposed the first prototype of valveless pump consisting of a circular cylindrical volume where the top side had a thin brass diaphragm to which a piezoelectric disc was fixed. Its flow rate was 15.6 ml/min. Olsson et al. (1995, 1996, 2000) investigated the flow-directing properties of several diffuser elements with different lengths and opening angles for valveless micro-pumps. Numerical simulations were done by using the Computational Fluid Dynamics program ANSYS/Flotran. Our study group also designed and simulated a valveless micro-pump which has a 0.5 mm thick chamber and a 20 degree open angle (Ma et al. 2006). The peak flow rate in the simulation was only 0.12 ml/min. In general, a valveless pump cannot provide a high flow rate in a closed system with high flow resistance. Therefore, a new design of a one-side actuating micro-diaphragm pump (Ma et al. 2007) is developed to actuate the liquid by the vibration of a diaphragm with a thinner structure and a higher flow rate.

## 2 Development of a piezoelectric micro-diaphragm pump

Generally, a diaphragm pump with passive check valves can overcome higher flow resistance and improve the performance. Ordinary micro-pumps cannot provide enough flow rates due to the limited actuating force by diaphragm's displacement. Böhm et al. (1999) developed a plastic micro-pump with a valve which is capable of pumping both liquid and gas at pump rates 2 ml/min for water and up to 50 ml/min for air when the actuation frequency is between 2 and 500 Hz. A commercial product of SDMP305D with central-actuating (Star Micronics Co. 2006), which is shown in Fig. 1, is a thin, compact, and lightweight micro-diaphragm pump. However, it is limited to the height, the control volume, and the mass flow rate due to its actuating displacement in  $z$ -direction by Piezoelectric effective. Its maximum flow rate is only 5 ml/min.

### 2.1 One-side actuating micro-diaphragm pump

In Fig. 3, a new micro-diaphragm pump with piezoelectric effect has been designed to actuate the working fluid by the vibration of a diaphragm with one-side sector-shaped

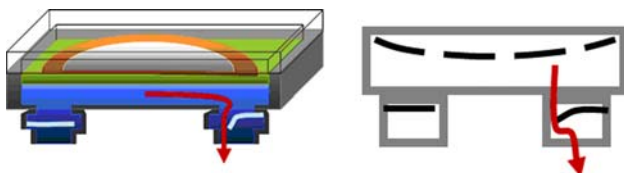


Fig. 1 View of SDMP305D micro-diaphragm pump

piezoelectric device. The vibration amplitude of a piezoelectric device produces an oscillating flow and alters the chamber volume by the curvature change of a diaphragm. While the actuator is moving downward to decrease chamber volume shown in Fig. 2a, the outflow will be in one direction with inlet valve closed and outlet valve open. While the actuator is moving upward to increase chamber volume shown in Fig. 2b, the inflow will be in the chamber with the inlet valve open and the outlet valve closed. The new design of the one-side actuating diaphragm pump with two check valves, which is shown in Fig. 3, allows the pump to be thinner and generates flow in one direction. In addition, the actuating force can be enforced by its harmonic resonance of the working fluid with the vibration of a rectangular piezoelectric device, PDMS diaphragm, and two check valves in the pump chamber.

### 2.2 Theoretical analysis

The passive check valve is an important device in a new design of one-side actuating micro-diaphragm pump. It decides the performance of the pump. The governing equation of oscillating motion for valves, which is shown in Fig. 4, can be expressed by Eq. (1)

$$m \frac{d^2y}{dt^2} + c \frac{dy}{dt} + ky = F \sin(\omega \cdot t) \quad (1)$$

where  $m$ ,  $c$ ,  $k$  are mass, damping coefficient, and spring constant, respectively. The right-hand term,  $F \cdot \sin(\omega \cdot t)$ ,

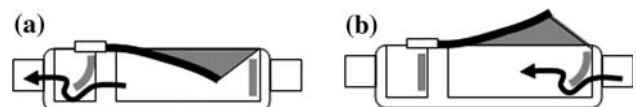


Fig. 2 One-side actuating micro-diaphragm pump

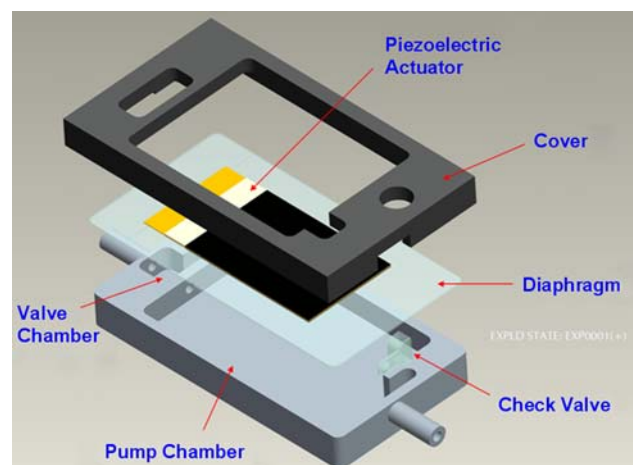


Fig. 3 Newly designed micro-diaphragm pump

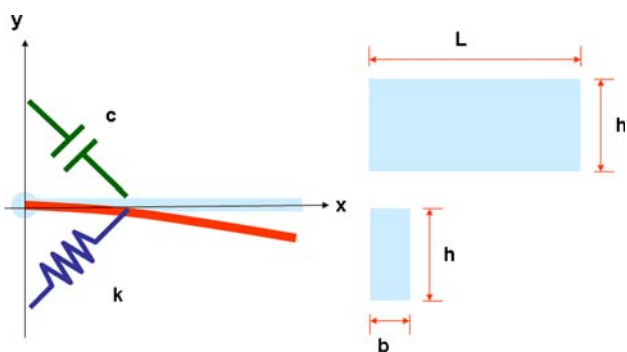


Fig. 4 A single degree-of-freedom system

represents the external force from actuating diaphragm acting on the valve.  $\omega = 2\pi f$  is the frequency of the piezoelectric device. The left-hand side of the equation describes the force from the system components that comprise a single degree-of-freedom system. The inertia force of valve with mass  $m$  is the change rate of linear momentum  $m \cdot a$ . The damping force generated by the viscous fluid is proportional to the pressure drag and friction drag. The damping factor  $\zeta$  is defined as

$$\zeta = \frac{c}{2\sqrt{k \cdot m}} \tag{2}$$

The damping factor is a function of the shape of the valve, the kinematic viscosity of the fluid, and the frequency of oscillation of the valve. Check valves are manufactured from PDMS. It is a flexible, transparent elastomer ideally suited for electrical/electronic potting and encapsulating applications. The elastomer is elastic structural element which can be expressed as spring motion to store and release the energy. In this study, the shape of the check valve can be considered as a cantilever beam. The bending moment is a function of position along the valve, and the deformation of the valve is small. Thus, the differential equation for the elastic curve of the valve can be shown as:

$$EI \frac{d^2y}{dx^2} = M(x) \tag{3}$$

where  $E$  is the module of elasticity;  $I$  is the second moment of area of the transverse section with respect to the neutral axis; and  $M$  is the bending moment of the section. The spring constant  $k$  of the cantilever valve can be calculated from Eq. (3) as:

$$k = \frac{3EI}{L^3} \tag{4}$$

where  $L$  is the length of the valve, and  $I = bh^3/12$  is the second moment of area of a rectangular section.

For translation oscillations of the valve, the natural frequency  $\omega_n$  of the valve in vacuum is defined as:

$$\omega_n = \sqrt{\frac{k}{m}} \tag{5}$$

### 2.3 Head loss

For steady, inviscid, incompressible flow, the total energy remains constant along a streamline. The energy line also represents the total head available to the fluid. Consider the friction drag, the total head loss  $H_L$  can be calculated by the Bernoulli equation and be written as

$$\frac{P_1}{\rho g} + \frac{1}{2} \frac{v_1^2}{g} + z_1 = \frac{P_2}{\rho g} + \frac{1}{2} \frac{v_2^2}{g} + z_2 + H_L \tag{6}$$

Both the pressure of the inlet  $P_1$  and the outlet  $P_2$  are the atmospheric pressure. The total head loss may further be reduced by neglecting the inlet velocity  $v_1$  and setting  $z_2$  as zero.

$$H_L = z_1 - \frac{1}{2} \frac{v_2^2}{g} \tag{7}$$

### 2.4 Manufacture

The micro-diaphragm pump chamber is fabricated in an aluminum case by using highly accurate CNC machine, and the cross-section dimension is 28 mm × 5 mm (without cover). Both check valves and diaphragm are manufactured from PDMS. PDMS (SYLGARD 184 silicone elastomer) is supplied in two parts, a lot-matched base and curing agent mixed in a ratio of 10 parts base to one part curing agent by weight. PDMS congeals at 25°C in 24 h, and becomes full solid in 7 days. Besides, it congeals in thick or thin section to a flexible, transparent elastomer ideally suited for electrical/electronic potting and encapsulating applications.

A rectangular piezoelectric device is chosen as the actuator in our study, and its dimension is 0.6 mm × 20 mm × 40 mm. The performance of the piezoelectric device varies depending on the mounting and driving conditions. The blocking force of the piezoelectric device mounting on one side is less than 0.4 N in zero deflection, and the amplitude of the piezoelectric device is less than 0.5 mm without loading, when the free length and input voltage are 33 mm and ±50 V.

The inlet and outlet check valves are placed in the valve chamber after they solidify. Then, the diaphragm and the case are glued by the liquid mixture of PDMS. In order to expedite the process, the PDMS in the pump will be heated

to congeal in an oven. Finally, the piezoelectric device is fixed on the diaphragm.

### 3 Experimental set-up

Figure 5 shows the experimental setup for the performance test of the micro-diaphragm pump. The micro-diaphragm pump with a piezoelectric device is driven by an alternating sine-wave voltage of  $\pm 50$  V at 70–180 Hz. The signal waves and frequencies are controlled by a function-generator. An amplifier is needed to modulate the voltage to the specific dB and the input signals can be monitored by an oscilloscope. The water flow rate data are recorded every 10 Hz to analyze the pump performance in different potential heights and operating conditions.

Without activating the pump, certain flow velocities through the whole system are obtained by adjusting the water level. As shown in Fig. 6, the resistance in the pump ( $H_{\text{pump}}$ ) can be calculated by the total head loss of the whole system ( $H_L$ ) minus the head losses from  $H_{\text{coldplate}}$  and  $H_{\text{pipe+other}}$ . The resistance in the cold plate ( $H_{\text{coldplate}}$ ) can be measured by the similar way.

The system is a close loop as there is no air either in the pipe or the components, as shown in Fig. 7. The interface of the cold plate and the dummy heater is smeared with thermal grease. Then, the cold plate and the dummy heater are fixed together with screws by a torque wrench. In order to improve the dissipation efficiency of the radiator, a fan of  $12\text{ V} \times 0.3\text{ A}$  is applied on the radiator. The power input of the micro-diaphragm pump is an alternating signal of  $\pm 50$  V at 90 Hz. In addition, the temperature variations of the heater are to be recorded from 20 W, and then continuously be recorded every 5 watts until 60 W.

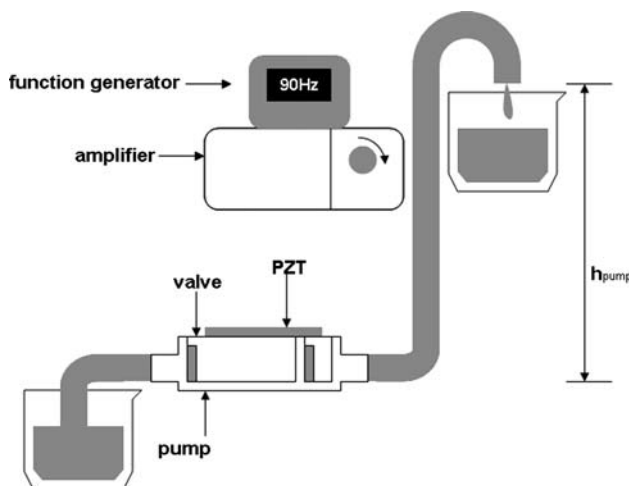


Fig. 5 Set-up for pump performance

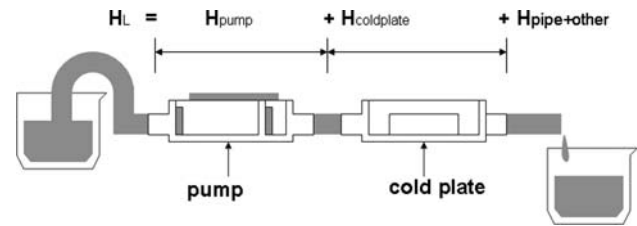


Fig. 6 Set-up for resistance measurement

## 4 Results and discussion

### 4.1 Effects of actuating frequency on flow rates

The flow rate gradually rises as frequency increases in a well designed pump. However, most of the flow rate–frequency curves (Figs. 9, 10) show two or more peak values at different frequencies in different designs. A very low flow rate at a higher frequency may occur in bad designs. This is enormously relevant to the vibration amplitude of the piezoelectric device which may produce oscillating flows by altering the curvature of a diaphragm. The flow rate drops correspondingly if the valve does not function properly as the actuator moves downwards and upwards in order to change the chamber volume. In an abnormal actuating operation shown in Fig. 8, the outlet valve may not be able to avoid back flow as the actuator vibrates at a certain frequency as the control volume changes. The motion of the outlet valve which mismatches

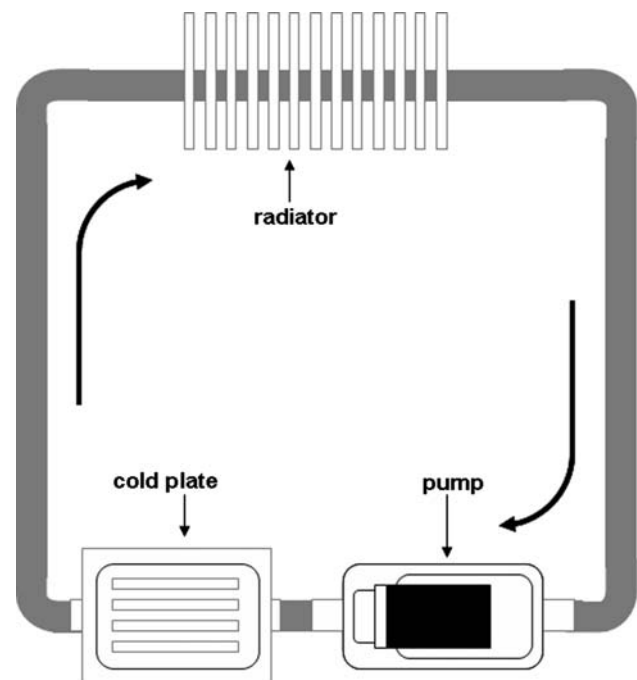
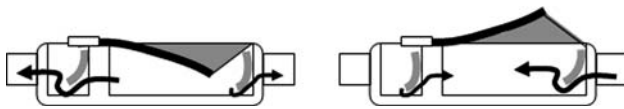


Fig. 7 Experimental set-up for performance test in a NB water cooling system



**Fig. 8** Phenomena in abnormal actuating cases

the vibration of membrane may cause the inability to produce a net outflow.

#### 4.2 Effect of diaphragm valve thickness

In general, the oscillating flow generated by the piezoelectric device can be affected by changing the thickness of a diaphragm. A thinner diaphragm will deform unpredictably by the actuator. Consequently, the change of the control volume decreases or even becomes zero. This causes the deactivation of the pump. On the contrary, a thicker membrane has larger tension. The actuator has to overcome the tension of the membrane as well as to drive the working fluid in the pump. In this study, the dimension of a standard valve is 5 mm × 3 mm, and the standard diaphragm is 0.03 g/cm<sup>2</sup>.

Figure 9 is the comparison of measured flow rate profiles obtained under different valve thicknesses. Obviously valve thickness has large influence on the flow rate. The higher flow rates may occur at frequency 130 and 180 Hz by using thickness 0.5 mm valves. The resonance phenomenon happens in the pump chamber due to the vibration of the working fluid with the system components (valve, diaphragm). The resonance frequency determines where the highest flow rate locates. Usually the valve is constrained by viscosity and inertia force caused by the working fluid. Under a fixed inertia force, the thicker the valve is, the smaller the response acceleration will be; that is, the smaller displacement will be made. The small gap between the outlet pipe and the valve causes high resistance in flow and thus results in reducing the flow rate. A similar phenomenon exists in different valve thicknesses.

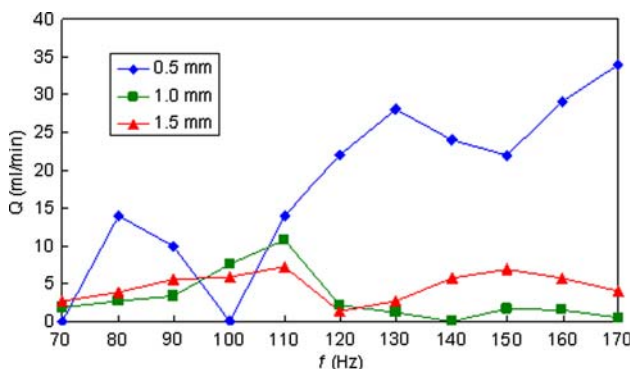


**Fig. 9** Measured flow rate with different valve thicknesses at different frequencies (under ±50 V)

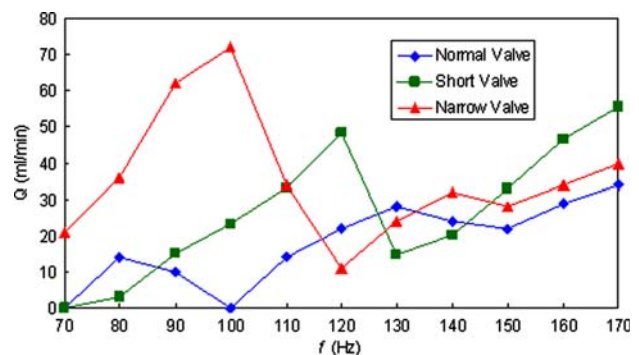
#### 4.3 Effect of valve length and shape

Figure 10 is the comparison of measured mass flow rate profiles obtained under different types of valve. Obviously the valve length and shape also have large influence on the mass flow rate. The pump performance can be improved if the outlet valve is replaced with a shorter one. The local maximum flow rate with the short valves is 48 ml/min at 120 Hz. Furthermore, the narrow-type valve may lead to a higher flow rate, which is 72 ml/min at 120 Hz, due to a smaller mass and lower drag resistance. The drag coefficient of a valve depends on its shape and the viscosity of the fluid.

In addition, the deflection of the piezoelectric device depends on the input voltage, and it also directly affects the flow rate. The characteristics of the pump with narrow valves from 90 to 110 Hz are shown in Fig. 10. The maximum flow rates (under ±50 V) of the three conditions are 62, 72, and 34 ml/min, respectively. The flow rate is proportional to the input voltage when the voltage is lower than ±20 V. In Fig. 11, the Q–V curve of 110 Hz remains proportional to input voltage after ±20 V, whereas the other two curves climb up more gradually after ±20 V until ±50 V, especially at 100 Hz.

#### 4.4 Pump performance under certain pressure heads

Pump performance changes when applied with different pressure heads. The H–Q characteristic of our pump design with thickness 0.5 mm narrow valves at three different frequencies (90–110 Hz) is shown in Fig. 12. The pressure head represents the height of the pipe outlet above the pump. The flow rate varies with the pressure heads as shown in Fig. 5; it also decreases linearly while pressure heads increase. Moreover, a higher flow rate in the Q–f curve can also provide a higher pump head in H–Q curve in the same pump. The flow rate at 100 Hz approaches to zero when the pressure head is 0.52 m.



**Fig. 10** Measured flow rate with different valve type at different frequencies (0.5 mm thickness under ±50 V)

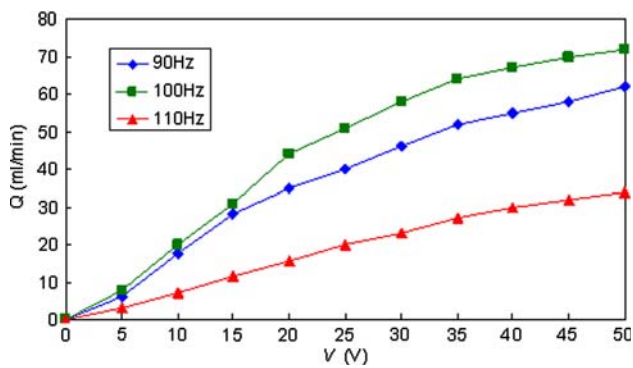


**Fig. 11** Measured flow rates at different voltages (with thickness 0.5 mm narrow valves)

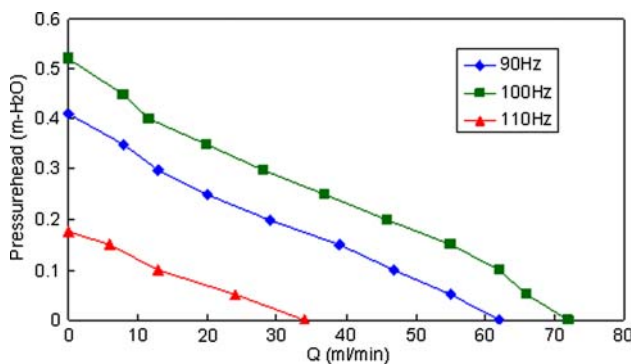


**Fig. 12** H–Q curves of the micro-pump (with thickness 0.5 mm narrow valves)

#### 4.5 Head losses in a system

Figure 13 shows the head losses in the system, pump and cold plate linearly increase with the flow velocity. The total pipe length in the system is 0.77 m. The resistance in the pump is the major head loss in the whole system. The results also show the fact that the head loss is proportional to the flow velocity because one-side micro-diaphragm pump has higher power to actuate water through the system.

### 5 Application of micro-diaphragm pump in a closed water cooling NB system

In recent years, temperature control of electronic devices has become more important because heat dissipation has increased substantially, due to the device miniaturization, increased heat flux in gaming notebook computer (NB), and workstation NB. Increasing temperature directly affects the performance and reliability of a device. Therefore, the thermal management plays a vital role for Central Processing Unit (CPU) and Graphics Processing Unit (GPU) in NB design.

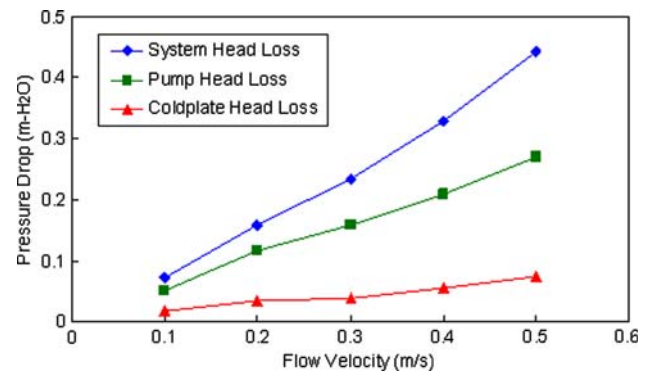


**Fig. 13** Head losses of components (thickness 0.5 mm pump valves)

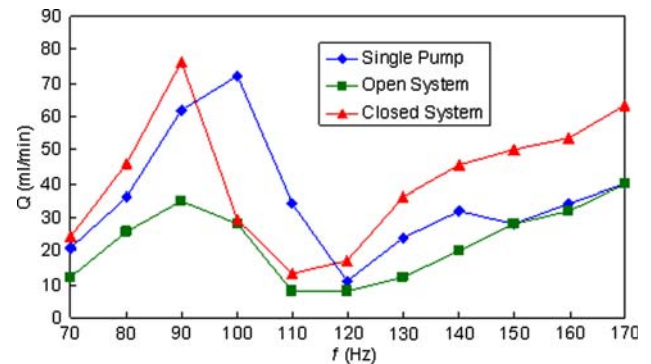


**Fig. 14** The comparison of pump flow rates in different frequencies at several systems

This study focus on the performance of a micro-diaphragm pump applied in a closed water cooling system, with a simple design of a cold plate and a radiator in the testing system. The flow rate in the closed system is measured by the movement of a small bubble along the pipe. The bubble speed is recorded at several operation frequencies. Therefore, the flow rate can be obtained by substituting the velocity and pipe diameter (2 mm) into  $\pi r^2 v$ . Figure 14 shows the flow rates comparison between the pump and closed system. The flow rate drops when the pump operates in the open system (as shown in Fig. 6) due to the head loss of the components. However, a higher flow rate is observed in the closed system due to energy preserving in the loop. The fluid element gains the momentum at the pump, and it retains part of the momentum after returning to the pump. In addition, the frequency of the highest flow rate shifts left, i.e., the maximum flow rate occurs earlier.

The relation between the heat generated in a dummy heater and its core temperature is considered. The measured results (Fig. 15) show that the designed cooling system keeps a core temperature in the dummy heater at 48°C during a 30 W operation. It is a sufficient resolution to the heat releasing of present laptops on full speed

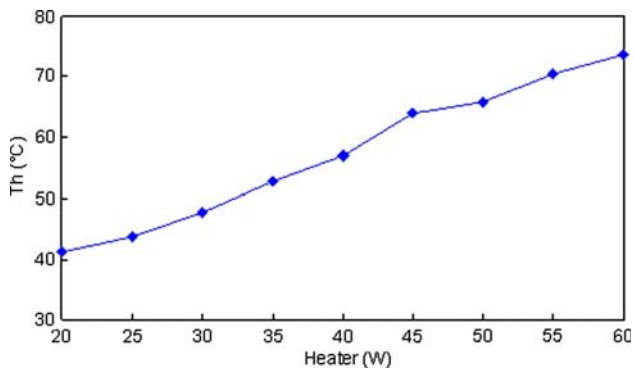


**Fig. 15** Thermal performance of the water cooling system in a close loop (thickness 0.5 mm narrow valves)

operation. The result also shows the core temperature rises as its operation power increases. When the power reaches 60 W, the core temperature is 73.6°C.

## 6 Conclusions

A new design of a one-side actuating micro-diaphragm pump with a piezoelectric device has been successfully developed by making use of its harmonic resonance of the working fluid with the system components (valve, diaphragm) in the pump chamber. Its performance is affected by the design of check valves, diaphragm, piezoelectric device, chamber volume, voltage and frequency. It shows the following conclusions:

1. The measured maximum flow rate of a newly designed pump is 72 ml/min at zero pump head in the range of operation frequency 70–180 Hz.
2. Narrow valve with 0.5 mm thickness is an optimal value for higher pump flow rate, and the maximum voltage of a piezoelectric device is  $\pm 50$  V (AC).
3. The head of the micro-pump with narrow valves can reach 0.52 m.
4. The pump in a closed system generates higher flow rates than a single pump.
5. The newly designed micro-pump will be widely tested with the advantages of thin size, powerful flow rate, less leaking problem, and durability in the fields of closed system, heat dissipation, and fuel cell system in the future.

## References

- Benard WL, Kahn H, Heuer AH, Huff MA (1998) Thin-film shape-memory alloy actuated micropumps. *J Microelectromech Syst* 7:245–251
- Böhm S, Olthuis W, Bergveld P (1999) A plastic micropump constructed with conventional techniques and materials. *Sens Actuators A77*:223–228
- Francais O, Dufour I, Sarraute E (1997) Analytical static modelling and optimization of electrostatic micropumps. *J Micromech Microeng* 7:183–185
- Koch M, Harris N, Evans AGR, White NM, Brunnschweiler A (1998) A novel micromachined pump based on thick-film piezoelectric actuation. *Sens Actuators A70*:98–103
- Li B, Chen Q, Lee DG, Woolman J, Carman GP (2005) Development of large flow rate, robust, passive micro check valves for compact piezoelectrically actuated pumps. *Sens Actuators A117*:325–330
- Ma HK, Hou BR, Wu HY, Lin CY, Gao JJ (2007) Development of an one-side actuating micro-diaphragm pump with piezoelectric device. In: *Proceedings of 23rd IEEE SEMI-THERM Symposium*, pp 184–189
- Ma HK, Hou BR, Wu HY, Lin CY, Gao JJ (2006) Development of a micro-diaphragm pump with piezoelectric device. Report to Cooler Master Co.
- Olsson A, Stemme G, Stemme E (1996) Diffuser-element design investigation for valve-less pumps. *Sens Actuators A57*:137–143
- Olsson A, Stemme G, Stemme E (2000) Numerical and experimental studies of flat-walled diffuser elements for valve-less micropumps. *Sens Actuators A84*:165–175
- Olsson A, Enoksson P, Stemme G, Stemme E (1995) A valve-less planar pump in silicon. In: *The 8th international conference on solid-state sensors and actuators*, vol 2, pp 291–294
- Saggere L, Hagood NW, Roberts DC, Li HQ, Steyn JL, Turner K, Carretero JA, Yaglioglu O, Su YH, Mlcak R, Spearing SM, Breuer KS, Schmidt MA (2000) Design, fabrication, and testing of a piezoelectrically driven high flow rate micro-pump. In: *Applications of ferroelectrics, proceedings of 12th IEEE international symposium*, vol 1, pp 297–300
- Suzuki H, Yoneyama R (2003) Integrated microfluidic system with electrochemically actuated on-chip pumps and valves. *Sens Actuators B6*:38–45
- Stemme E, Stemme G (1993) A valveless diffuser/nozzle-based fluid pump. *Sens Actuators A39*:159–167
- Star Micronics Co. (2006) User's menu of SDMP305D micro-diaphragm pump, pp 2–3
- Takao H, Miyamura K, Ebi H, Ashiki M, Sawada K, Ishida M (2003) A thermo-pneumatic in-channel microvalve with PDMS diaphragm for integrated blood examination system on silicon. In: *The 12th international conference on solid-state sensors, actuators and Microsystems*, vol 1, pp 139–142
- Teymoori MM, Abbaspour-Sani E (2005) Design and simulation of a novel electrostatic peristaltic micromachined pump for drug delivery applications. *Sens Actuators A117*:222–229
- Yang KS, Chen IY, Chien KH, Wang CC (2004) A numerical study of the nozzle/diffuser micro-pump. In: *International conference on MEMS, NANO and smart systems*, pp 104–109